Top-down processing mediated by interareal synchronization

Astrid von Stein*[†], Carl Chiang[†], and Peter König*[†‡]

*Institute of Neuroinformatics, Winterthurerstrasse 190, CH-8057 Zürich, Switzerland; and [†]Neurosciences Institute, 10634 J. J. Hopkins Drive, San Diego, CA 92121

Perception and cortical responses are not only driven "bottom-up" by the external stimulus but are altered by internal constraints such as expectancy or the current behavioral goal. To investigate neurophysiological mechanisms of such top-down effects, we analyzed the temporal interactions of neurons on different levels of the cortical hierarchy during perception of stimuli with varying behavioral significance. We found that interareal interactions in a middle-frequency range (θ and α; 4–12 Hz) strongly depend on the associated behavior, with a phase relationship and a layer specificity indicating a top-down-directed interaction. For novel unexpected stimuli, presumably processed in a feed-forward fashion, no such interactions occurred but high-frequency interactions (γ; 20–100 Hz) were observed. Thus corticocortical synchronization reflects the internal state of the animal and may mediate top-down processes.

interaction | oscillation | α frequency | γ | stimulus selection

The classical view of cortical information processing is that of a bottom-up process in a feed-forward hierarchy. However, there is psychophysical, anatomical, and physiological evidence that top-down effects such as expectancy or the behavioral goal play a crucial role in the processing of input stimuli (1–6). Little, however, is known about the underlying neurophysiological mechanisms. Because synchronous activity among neurons has been suggested to play a major role for visual processing (7), synchronization between different cortical areas along the hierarchy seemed a prominent candidate for mediating top-down effects. We thus investigated interareal interactions in behaving cats during perception of stimuli with different internal contexts.

Connections between cortical areas terminate with characteristic laminar distributions. Either they form synapses mainly in the granular layer (feed-forward type) or in the supra- and infragranular layers (feedback type); thus, cortical areas can be assigned to different levels of the hierarchy of the visual system (8, 9). For our experiments, we selected area 17, area 7, and area 5 (lateral division). Area 17 is part of primary visual cortex; area 7, relatively distant to area 17[§] shows visual and polysensory responses (10), and area 5, monosynaptically connected to area 7, shows sensory and sensory motor responses (11). Furthermore, their placement on the dorsal surface of the cortex allows well-controlled implantation of microelectrodes at different depth. We recorded from different laminae to gather information about feedforward and feedback projections (Fig. 1a). Three cats were trained to attend to moving visual stimuli. Two different visual stimuli were presented and the cats had to either respond by pressing a button (go stimulus) or not respond but continue tracking (no-go stimulus). Intermittently novel stimuli not eliciting a trained behavioral response were presented. Local field potentials were recorded bipolarly (Fig. 1b) and power and cross-correlation functions were computed between all channels during the various behavioral conditions. The analysis was performed separately for five different frequency bands (Fig. 1c) (see *Methods*). We investigated first whether synchronous activity can be observed between distant areas along the visual hierarchy; second, how synchronization differs when the stimulus is associated with a change in behavior or not; and third whether

expectancy or previous experience of a stimulus have an impact on synchronization of neuronal activity.

Methods

Behavioral Procedure. The animals were situated in a $30 \times 30 \times 80$ cm³-sized box, constructed as a Faraday cage. At one side, a transparent inset allowed viewing of a monitor. When the cat was attending the display, a trial was started. The first stimulus was a neutral mask (preparatory stimulus) moving slowly across the screen. The animal was trained to track the mask until at a random delay a second stimulus emerged. These stimuli were either an iconic drawing of a mouse or a lightly shaded rectangle, both about 8° in size. For each animal, one of the stimuli was assigned the "go stimulus," and the animal had to press a lever positioned in front of the right paw. On the other stimulus ("no-go stimulus"), the animal had to continue tracking. In either case, the animal was rewarded on correct performance. Behavior was classified into six categories. Only highly correct trials in the two best classes were included in the analysis. A highly correct performance (C1 and C2) was reached in 66, 77, and 86% (Cat L, T, and P, respectively) after 3–4 months. After animals were fully trained, novel stimuli were interspersed in the normal sequence of trained stimuli. Because no particular response was associated, the cat was rewarded for either response. Attention of the animal to the stimuli and their fixation were controlled online, as well as by videotaping and frame-by-frame off-line analysis. Attention was classified with a score adapted from ref. 12. Only fully attentive trials were included in the analysis. Positioning of the stimuli within the receptive fields was verified by testing the evoked responses, both in areas 17 and 7.

Electrodes and Surgery. Electrode arrays consisted of Teflon-coated platinum iridium wires with a diameter of 50 μm and an impedance of about 200 kΩ at 1 kHz. Four wires were aligned with a Teflon ring, arranged with their tips staggered in depth and glued together (Fig. 1a). The separation of neighboring electrode tips was 600, 400, and 800 μm. Two to seven of such "quattrodes" were chronically implanted in each cat in areas 17 and 7, and in one cat in area 5. Electrodes were placed according to Tusa *et al.* (13) in P3-L2 (area 17), A3-L9 (area 7), A11-L9 (area 5), on top of the gyri. The shortest wire was placed in the uppermost layer of the cortex, the longest on the border of layer 6 and the white matter, the two remaining were distributed over the remaining cortical layers (Fig. 1a). Correct placement of the electrode arrays was verified in histological slices (Nissl stain). In 87.5%, the electrode arrays entered perpendicular to the cortical
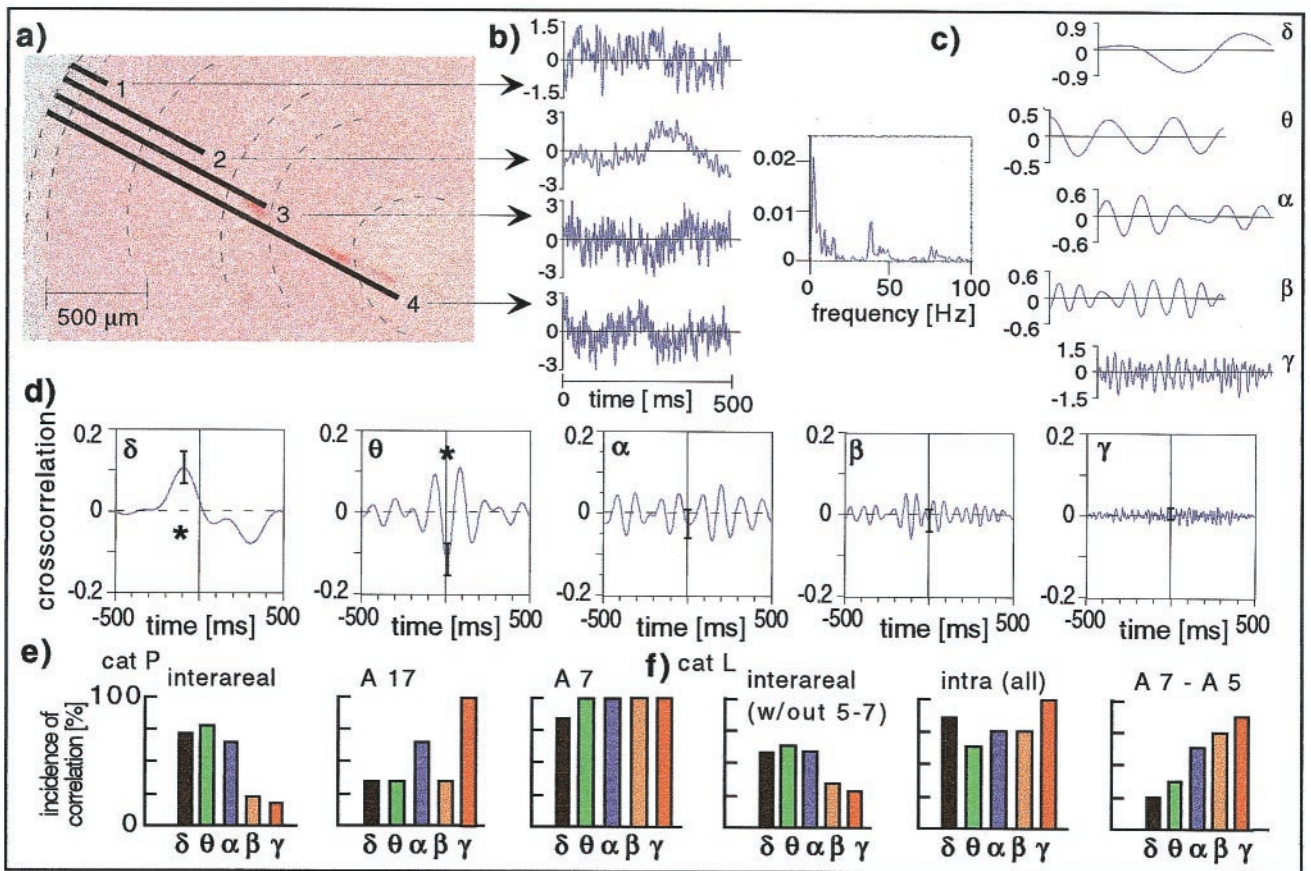

Fig. 1. Characteristics of intra- and interareal interactions. (*a*) Electrodes used. Electrode bundles had tips of varying length (here, area 17, Nissl stain). Electrode positions have been marked according to the lesions visible in the section shown as well as in adjacent sections. (*b*) Bipolar local field potentials were recorded from electrodes 1, 3, and 4 with respect to the electrode 2 (first, third, and fourth trace), and from electrode 2 with respect to a distant bone reference (second trace; this type of signal, however, is not further used in the present manuscript) (recorded epoch here, 500 ms during presentation of the no-go stimulus). (*c*) The power spectra of a single trial (bipolar electrodes 2 versus 3, third trace) is shown as an example. Because the power of the signal in the low-frequency ranges was dominant, analysis was separated into five frequency bands (δ, 2–4 Hz; θ, 4–8 Hz; α, 8–12 Hz; β, 12–20 Hz; and γ, 20–100 Hz). The filtered signals are shown (*Right*) by using the example of the third trace. (*d*) Cross-correlation functions of neuronal activity in two distant cortical areas. Cross-correlation functions of field potentials from the middle layer of area 17 and lower layers of area 7 (here, during presentation of the no-go stimulus). The star indicates significant cross-correlation functions ($P < 0.05$; $n = 125$). (*e*) Incidence of significant cross-correlation functions. Cross-correlation functions were determined for all electrode pairs in cat P and the incidence of significant cross-correlation functions is shown separately for the different frequency bands. Interareal interactions (area 17 - area 7, *Left*) and intraareal interactions (area 17, *Upper Right*; and area 7, *Lower Right*) are shown. Both go and no-go trials were considered. (*f*) The incidence of significant correlation functions (cat L). (*Left*) The incidence of significant cross-correlation functions determined for all interareal interactions excluding the pair with strong monosynaptic connections (area 5–area 7) is shown, together with the averaged incidence of significant intraareal cross-correlation functions (*Inset*). (*Right*) The interactions for the functionally neighboring areas 7 and 5 is shown. Both go and no-go trials were considered.

surface as planned. Data recorded by the remaining oblique electrodes were not used in the present manuscript; 75% of the longest wires of the arrays ended in the white matter or at the border with layer 6, and 25% were located in layer 6. Electrodes in area 17 were positioned slightly posterior to the representation of the area centralis, such that the center of the receptive fields were about 2° below fixation point. In addition, a silver ball electrode was placed epidural.

Data Acquisition. The bipolar local field potential was recorded by differential amplification of the signal from electrodes of a "quattrode" placed in different depth (14) (Fig. 1*b*). This measure appears as a reasonable compromise between, on one hand, recording with high spatial selectivity and on the other, sampling the activity of a large number of neurons for a statistically reliable signal. In addition, the potential at one electrode per bundle with respect to the silver ball reference electrode was recorded. The data were subjected to online filtering between 1 and 100 Hz, a 60-Hz notch filter was applied

to exclude line noise, and sampled at a rate of 1 kHz. During each session, the cat performed on average 120 trials lasting 7 s each.

Data Analysis and Statistics. Epochs of 500 ms aligned to onset of the event of interest (e.g., appearance of the second stimulus) were analyzed. Because the power of the signal in the lower-frequency ranges was dominant, analysis was performed separately in five different frequency ranges, chosen such that each band contained a similar amount of energy: 2–4, 4–8, 8–12, 12–20, and 20–100 Hz. These ranges are also in accordance with classical electroencephalogram conventions. The data were Fourier transformed and multiplied with the complex conjugate (cross- and autocomponents), and the inverse transformation was performed for selected, continuous frequency bins (corresponding to one "band"). In this way, we obtained autocorrelation and cross-correlation functions for separate frequency ranges. This procedure is equivalent to filtering in the frequency domain, which is an acausal and symmetric filter that causes least filtering artifacts such as phase distortion (15). Cross-correlation

functions were determined for single trials, normalized with the geometric mean of the autocorrelation coefficient of both signals, and averaged over trials. Such average cross-correlation functions differ from zero if oscillatory components of the two signals display a constant phase relationship over trials. The variance of these measures can be estimated with the error bars in Figs. 1d, 2 a and b, and 3. Finally, we determined the cross-correlation between two averaged evoked potentials; this procedure controls for the stimulus-locked component in a cross-correlation, as in the average potential internal relationships are lost and only phase relations to stimulus onset are maintained. This measure is closely related to the shift predictor (16). A cross-correlation was considered significant if the amplitude at the peak was at least 0.1 in size and significantly different from zero on the 5% level. The stimulus locked correlation (shift predictor) was nearly always flat and never explained a significant part of the observed couplings. For comparison of cross-correlation functions of selected electrode pairs during different stimulus types, we applied the Mann–Whitney rank sum test to the peak amplitudes. For comparing sets of electrodes, the paired Wilcoxon test was used. For the determination of phase shifts, only correlation functions significantly different from zero were considered. Phase shifts were determined by using the time lag at the maximal peak in the correlation functions. To gather information about second-order relationships between signals in different frequency ranges, we computed auto- and cross-bicoherence. We chose B_{xyx} (ω_1, ω_2) = < $X(\omega_1)Y(\omega_2)X(\omega_1 + \omega_2)$ > and B_{xyy} (ω_1, ω_2) = < $[X(\omega_1)Y(\omega_2)Y(\omega_1 + \omega_2)]$ > with $X(\omega_1)$ the Fourier transform of signal x at frequency ω_1 (window 500 ms aligned on stimulus onset, Hanning window, nonoverlapping) (for details, see refs. 17 and 18). B_{xxy} was computed for control. The significance of a bicoherence peak was estimated by assuming a discrete stochastic process, with real and imaginary part of the bispectrum being randomly distributed with equal variance (18). Because of the large number of points in the matrix, we used a significance level of 0.001.

Results

Characteristics of Inter- and Intraareal Interactions in Awake Animals.
Synchronization of neuronal activity was found between primary visual cortex (area 17) and a distant area in visual association cortex (area 7) in all three cats. Fig. 1d shows an example recorded during presentation of the no-go stimulus in cat P. Interestingly, the most prominent correlation between the areas was found in a middle-frequency range (θ, 4–8 Hz). This finding was supported by the overall statistics over electrodes as shown in Fig. 1e for cat P. Significantly correlated activity between the two distant areas (17 and 7) was found in the θ (78%), δ (73%), and α (67%) frequency range, and much lower in the γ-frequency range (17%). This is consistent with previous results in the monkey (19). In contrast, the distribution of significant cross-correlation functions of local interactions (within the two areas) was more evenly distributed or actually peaked in the γ-frequency range (Fig. 1e *Right*). Qualitatively similar results were found in cat L (Fig. 1f) and the other two animals. Thus, local interactions most consistently involved synchronous activity in the γ-frequency range (20), whereas long-range interactions involved middle and lower-frequency ranges.

Interactions of two areas with mostly monosynaptic connections were investigated in one animal (cat L) where additional electrode bundles had been implanted in area 5 lateral division (Fig. 1f *Right*). In contrast to the interactions between distant areas (area 17 - area 7; area 17 - area 5), the interactions between area 7 and area 5 were found most often in the γ-frequency range. This result is consistent with Roelfsema *et al.* (21) who report synchronization between area 7 and area 5 in the γ-frequency band. Synchronous activity in the γ-frequency range has also been reported between areas 17 and

PMLS in the cat and areas V1 and V2 in the monkey (22–25). These examples share the feature of strong monosynaptic connections between the investigated areas. Furthermore, also within one cortical area, the range of 7 to 10 mm where γ synchronization is found in primary visual cortex (7, 26–28) is of the same order of magnitude as the extent of tangential monosynaptic connections (29, 30). Thus, synchronization in the γ-frequency range might be viewed as a "local" phenomenon, limited to sites within an area or between two areas with strong monosynaptic connections. Middle-frequency couplings, on the other hand, can be found for long-range polysynaptic integration.

Effect of Behavioral Relevance on Interareal Interactions.
The interareal interactions were compared for similar stimuli but different behavioral significance, i.e., during go and no-go trials. Fig. 2a shows the cross-correlation of activity in area 17 with activity in area 7 during presentation of the two different stimuli in cat P. Comparing the two showed a specific difference in the θ, α (4–12 Hz) frequency ranges. Whereas the go-stimulus induced a significantly correlated activity at these two sites (red line, $P < 0.05$), during presentation of the no-go stimulus (blue line), no significant correlation between the areas was found. No such difference was found in the γ-frequency range (Fig. 2a *Right*). Thus, the stimulus which was associated with a change in behavior led to a specific increase of interareal coupling in the θ-, α-frequency ranges.

To dissociate physical stimulus properties and associated behavioral significance, in one animal (cat T), the assignment of stimuli to go and no-go paradigms was reversed (Fig. 2b). Similar to the other animals, the stimulus which was now the go stimulus induced a significant correlation between area 17 and area 7 in the θ-, α-frequency range (red line, $P < 0.05$), whereas the other stimulus (blue line), now used as the no-go stimulus, did not. Thus, interareal interactions are determined not just by the physical stimulus properties as such, but by the associated behavioral significance.

This result was found consistently in most electrode pairs. As a measure for changes in cross-correlation, Fig. 2c (black bars) shows the ratio of the cross-correlation amplitude during go and no-go stimuli. Each bar represents the average ratio over all electrode pairs in cat P for a particular frequency range. The figure shows that a significant difference between go and no-go stimuli, i.e., a ratio different from one, on average is observed, and that the ratio is larger than one, indicating an enhanced coupling during go-stimuli with respect to no-go stimuli. The enhancement was most prominent and significant in the α-frequency range ($P < 0.05$). During an unspecific stimulus preceding the target stimulus (preparatory stimulus, gray bars), as expected, no difference between the two types of trials was observed in the cross-correlation amplitude.

A qualitatively similar picture emerged for all cats examined in this paradigm. In cat T, the maximum difference between go and no-go stimuli was found in the α (go/no-go ratio 1.44) and θ-frequency band (go/no-go ratio 1.41); in cat L, it was at θ-frequency (go/no-go ratio 1.25). These enhancements of go versus no-go correlation amplitudes were significant with $P < 0.05$ in all animals.

In summary, processing of visual stimuli that require a change in behavior was accompanied by a prominent interaction between area 17 and area 7 within the first 500 ms of stimulus-presentation in all examined cats. These interactions took place in the middle (θ, α)-frequency ranges.

Largely synchronized middle-frequency cortical activity has been reported in electroencephalogram scalp recordings and is usually attributed to states of inattentiveness or absence of cortical input (alpha rhythm) (31, 32). Therefore, our finding of middle (θ, α)-frequency synchronization between primary visual cortex and parietal cortex raises questions regarding nonspecific arousal effects. First, go and no-go trials were balanced for their attention, because only trials with high attention score were included in the
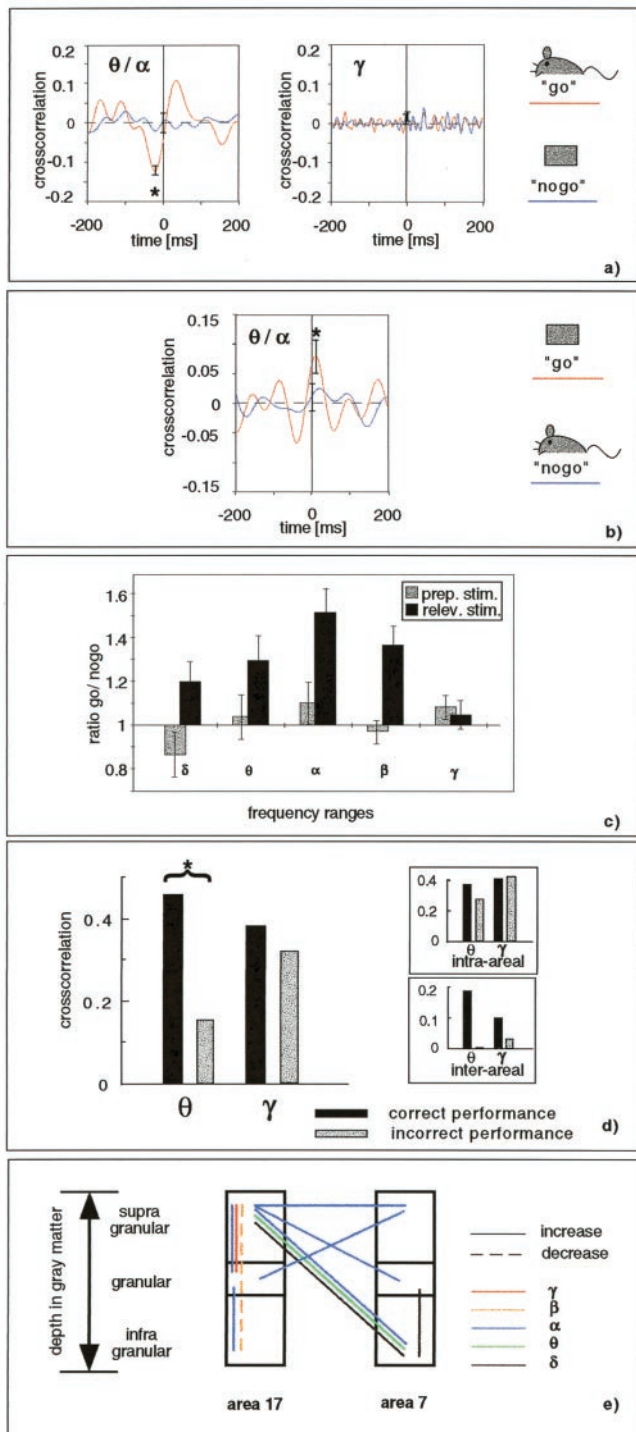
analysis. Second, if the middle-frequency synchronization during go stimuli would reflect inattentiveness, then we would expect an even higher degree of synchronization during incorrect trials. However, to the contrary, the cross-correlation in the middle-frequency range in trials with incorrect performance was significantly lower than in trials with correct performance (Fig. 2*d*, cat L). A qualitatively similar result was observed in all examined animals (frequency band with maximal observed difference between correct and incorrect trials: cat P, α; and cat T, θ). Within the incorrect trials, we observed a tendency of false-negative trials showing even lower cross-correlations than false positive, which, however, because of the low number of trials in such a breakdown did not reach significance. These results demonstrate that interareal interactions in the middle-frequency range are actually related to the successful processing of stimuli.

Direction of Interaction Between Visual Areas. To gather insights in the direction of interaction between the areas on different levels of the hierarchy, we used several indirect approaches. The relative timing of activity at two sites was determined by computing time shifts of neuronal activity. In the γ-frequency range, the time lag of the peak in the cross-correlation function was on average smaller than 2 ms, i.e., an order of magnitude smaller than the period length (Table 1). Furthermore, time lags showed a clear unimodal distribution with a peak at zero. This matches results obtained in the anesthetized preparation, where γ activity between neurons was nearly perfectly synchronized (24, 33). In contrast, interactions in the θ-, α-frequency ranges were associated with larger time lags, ranging from 12 to 31% of period time (taken at the center of the band with the largest effect; Table 1). Furthermore, the distribution of time lags showed peaks off zero. Thus, only middle-frequency interactions showed large time lags between the recorded sites. The direction of interaction can be obtained if the sign of the lag is considered. If time lags are investigated exclusively for the interactions between area 17 and area 7 (Table 1), for each animal, the average time lag is negative, indicating that the activity in area 7 leads that in area 17. Interestingly, this tendency was significantly present only during go stimuli ($P < 0.05$). No systematic time lags were found during presentation of no-go stimuli. This result suggests that during go stimuli, area 7 was leading area 17, compatible with a feedback influence.

With a sliding window (width 200 ms; step size 50 ms), we compared the development of activity and correlation. Within the resolution of the method, we did not find a difference between the time courses. In particular, no "flow of activation" was observed in the top-down direction. Thus, we have to differentiate between activating and modulating influences; the lead of area 7 observed in the correlations has to be interpreted as being of modulating type (compare ref. 34).

Further insights into the direction of interaction might be gathered by considering the laminar patterns of interareal correlations and comparing them to the termination pattern of feedforward and feedback connections. Fig. 2*e* shows the laminar distribution of the

Fig. 2. (*a*) Cross-correlation between supragranular layers of area 17 and infragranular layers of area 7 in the middle-frequency range (4–20 Hz, *Left*) during presentation of the go (red line) and no-go (blue line) stimuli. The star indicates a significant cross-correlation during go trials ($P < 0.05$, $n = 75$). The respective cross-correlation functions in the high-frequency range are shown (*Right*). (*b*) In one cat, stimuli for go and no-go trials were reversed (icons to the right). The cross-correlation of neuronal activity in area 17 and area 7 is shown for either stimulus. The star indicates a significant cross-correlation during go trials. (*c*) As measure for an enhancement of cross-correlation, the ratio of cross-correlation amplitudes during go and no-go trials is introduced. It is averaged over all electrode pairs (cat P). Black bars, ratio during the relevant second stimulus; and gray bars, ratio during the preparatory first stimulus. A significant enhancement of cross-correlation (i.e., a ratio > 1) is found with a maximum at alpha frequency; this difference between go and

no-go cross-correlation was significant ($P < 0.05$) in a paired Wilcoxon test. (*d*) Comparison is shown of cross-correlation during stimulus presentation in correctly performed go trials and incorrectly performed trials (average over all electrodes of area 17 and 7, cat L). The star indicates a significant difference in the θ-frequency range between correct and incorrect trials ($P < 0.05$, paired Wilcoxon test). The small difference seen in the γ range did not reach significance. The inlet shows the subdivision into intraareal and interareal interaction, demonstrating that a substantial increase is accounted for by the interareal interactions. (*e*) Electrode-pairs where cross-correlation differed significantly ($P < 0.05$) between go and no-go stimuli are depicted with respect to their position in the different cortical layers (cat P). Solid lines, increased cross-correlation during go stimuli; and dashed lines, decreased cross-correlation during go stimuli. The different frequency ranges are indicated by color.

Table 1. Time lags of interactions

Phases	θ/α, ms	γ, ms
Cross-correlation-absolute phases		
Cat L	50.7 ± 9.1	0.7 ± 0.1
Cat T	20.8 ± 8.2	0.7 ± 0.2
Cat P	18.2 ± 3.1	1.9 ± 0.3
Interareal phases (go stimuli)		
Cat L	−58.0	
Cat T	−29.0	
Cat P	−16.4	

For cross-correlation, average absolute time lags were determined for all significant cross-correlation functions for both types of stimuli (go and no-go) in the θ/α and γ frequency ranges. The substantial difference between phase-lagged cross-correlation in the θ/α frequency range and synchronized activity in the γ frequency range was present also when separate analysis of go and no-go stimuli was performed (data not shown). For interareal phases, the time lags were computed during go stimuli for the interareal interactions only. Averaged over electrodes, a significant negative time lag was observed in all animals ($P < 0.05$). In contrast, no statistically significant bias was observed during the presentation of no-go stimuli.

behavior-specific changes in cross-correlation of activity. Most prominent is the coupling between the infragranular layers of area 7 and the supragranular layers of area 17. This distribution matches the laminar distribution of the feedback connections (35). An influence of feedback projections on the activity in the superficial cortical layers of the primary visual cortex has been shown in different paradigms (3, 5, 36–38). Thus, the laminar distribution of the behavior-specific cross-correlations is compatible with an effect mediated by feedback connections.

The two arguments developed above concentrate on the anatomical and physiological levels. To address the issue of the direction of interaction on the functional level, a modified behavioral paradigm was used in one animal. In the pseudorandom sequence of trained go and no-go stimuli, novel stimuli were interspersed. The cat usually was very attentively watching those stimuli. Stimuli had neither been seen before nor was a specific motor response associated, and thus presumably the processing of these unexpected stimuli could not be primed by top-down signals. In contrast to the strong middle-frequency correlations found during presentation of known stimuli, these novel stimuli did not induce a significant cross-correlation in the middle-frequency ranges (Fig. 3). In contrast, interactions in the γ-frequency range were of similar size in the two conditions, even with a tendency of an increase during the novel stimuli. This result suggests that when top-down interactions do not contribute to processing, interareal interactions in the middle-frequency range are much reduced. Thus, cortical synchronization is influenced by experience and expectation reflected in the internal state of the animal. Interestingly, synchronized activity on a ms time scale has been found during the preparatory phase in monkey parietal cortex (39). The tendency of interactions in the γ-frequency range to increase for novel stimuli, on the other hand, supports the hypothesis that synchronization in the γ-frequency range is relevant for bottom-up processing and with its precise timing of neuronal activity is particularly important for learning and plasticity (40, 41).

Taken together, these three approaches suggest a contribution of top-down-directed interaction in the processing of the behaviorally relevant visual stimuli expressed in the synchronization of neuronal activity. Certainly, this interpretation has to be taken with due caution because we have investigated only a small part of the complete network involved in the process of perception and sensory motor reaction. Investigation of the complete system would be necessary to decide whether the correlated activity between areas 17 and 7 indeed reflects a feedback from areas 7 to 17, or whether both are driven by other areas. Pilot studies with autoregressive methods, however, show (42) that the activ-
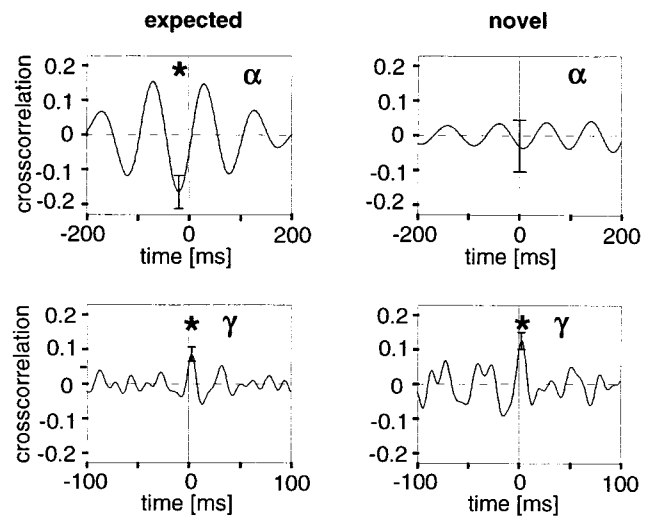

Fig. 3. Interareal interactions during presentation of a trained stimulus ($n = 73$) and a novel stimulus ($n = 34$). Cross-correlation functions are shown for the α-frequency (*Upper*) and γ-frequency (*Lower*) ranges. The stars indicate a significant correlation in the α-frequency range during presentation of the expected stimulus ($P < 0.05$) but not the unexpected stimulus (the difference between the two is significant with $P < 0.05$), and in the γ-frequency range during presentation of expected as well as novel stimulus (both $P < 0.05$).

ity in area 7 helps to predict activity in area 17, which is indicative for a causal interaction (43).

Phase Coupling Between Activity in the γ and θ-, α-Frequency Range. These findings suggest a role of θ-, α-frequency interactions in top-down processing, whereas γ-frequency interactions have been related to external stimulus properties (7) and thus might play a role in bottom-up processing. Because an integration between bottom-up processing and top-down processing seems a necessary step for successful perception and sensorimotor integration, one would expect some kind of coupling between γ-frequency activity and θ-, α-frequency activity, in particular
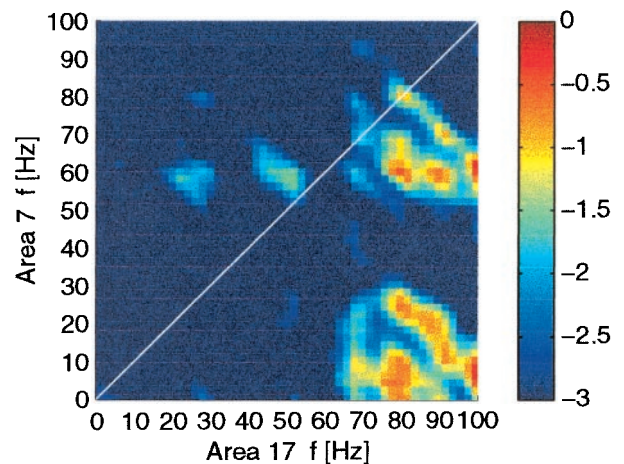

Fig. 4. Phase coupling between different frequency components. Cross-bicoherence was computed between the signals in area 17 (*x* axis) and area 7 (*y* axis) during the go stimuli. Shown is the smoothed logarithm of the bicoherence values. The peak in the lower right corner indicates a phase coupling between γ (60–100 Hz) activity in area 17 and 0–30 Hz activity in area 7. This peak (bicoherence at 80 × 8 Hz, 0.6) was significant with $P < 0.001$.

von Stein *et al.*

during processing of behaviorally relevant stimuli. We therefore used bicoherence analysis, a method to investigate phase coupling between different spectral components of one (autobicoherence) or two (cross-bicoherence) signals (17, 18, 44).

A prominent phase coupling was found in the interareal bicoherence. Here, major peaks of phase coupling were present between γ frequencies of area 17 and θ, α frequencies of area 7 (Fig. 4). Such asymmetric coupling of higher frequencies in area 17 with lower frequencies in area 7 was seen in 67% of the interareal electrodes. The tendency of asymmetric coupling was only seen for the cross-bicoherence between different areas; intracolumnar bicoherence and autobicoherence showed no such tendency. Comparing bicoherence during go and no-go stimuli showed that the asymmetric coupling between high frequencies and low frequencies was only present during go stimuli. During no-go stimuli, coupling was more symmetric or showed no peaks at all.

Thus, analysis of the higher-order spectral components gives evidence that there is a phase coupling between γ frequencies in area 17 and θ, α frequencies in area 7, which is in accordance with the hypothesis that γ frequencies reflect bottom-up processing and lower frequencies reflect top-down processing. Furthermore, this coupling was specific for stimuli that were associated with behavioral relevance.

Discussion

Summarizing, we found significant interactions between areas along the visual hierarchy. Whereas interactions in the γ-frequency range were found predominantly locally, i.e., between sites within the range of monosynaptic connections, interactions between distant cortical areas evolved mainly in the middle (4–12 Hz)-frequency ranges. Thus, the range of a functional interaction seems to have an impact on the frequency of an oscillatory process (45). Gamma interactions had a tendency to increase during novel stimuli and thus might be related to bottom-up processing and mechanisms of learning and plasticity, in line with their dependence on Gestalt properties of stimuli (7). Middle-frequency interactions depended on the behavioral significance of stimuli. Furthermore,

they were related to stimulus expectancy. Because also the relative timing of activity and the laminar pattern of cross-correlation functions during these periods indicated a top-down-directed interaction, we suggest that middle-frequency interaction might mediate top-down processes. This view is compatible with and extends the classical notion of the middle frequencies as idling rhythm of the brain (alpha rhythm) (31, 32). States which show maximal alpha activity as, e.g., when the eyes are closed, may reflect states of the visual cortex (46) without bottom-up input (in this respect, "idling"), but with purely internal mental activity such as during imagery, thinking, or planning. Thus, the alpha rhythm may be taken as an extreme example of top-down processing. Indeed, enhanced α or θ interactions have been found in cats during states of intense expectancy (47). Furthermore, visual cortical background activity of neuronal spiking [predominant in the middle-frequency ranges (50)] has been shown to have a major influence on processing of bottom-up input (51). Therefore, middle-frequency interactions seem a suitable candidate for top-down processes as proposed by the results of this study. It is tempting to relate these different phenomena to different cellular substrates. Indeed, cellular activity of both frequencies are found, i.e., neurons intrinsically bursting with γ (20–70 Hz)-frequency (52) and neurons firing with α (around 10 Hz) frequencies (49, 53). However, the observed coupling of frequencies also points to the importance of network effects. Top-down middle-frequency interactions seem to be integrated and phase coupled with bottom-up γ-frequency interactions during successful processing of stimuli that are associated with behavioral relevance. Concluding, cortical synchronization seems not only driven by external stimulus properties, but additionally by top-down influences such as the cat's learned associations with a stimulus and the actual behavioral context and expectancy.

1. Moran, J. & Desimone, R. (1985) *Science* **229,** 782–784.
2. Motter, B. C. (1993) *J. Neurophysiol.* **70,** 909–919.
3. Le Bihan, D., Turner, R., Zeffiro, T. A., Cuenod, C. A., Jezzard, P. & Bonnerot, V. (1993) *Proc. Natl. Acad. Sci. USA* **90,** 11802–11805.
4. Kastner, S., Nothdurft, H. C. & Pigarev, I. N. (1997) *Vision Res.* **37,** 371–376.
5. Hupe, J. M., James, A. C., Payne, B. R., Lomber, S. G., Girard, P. & Bullier, J. (1998) *Nature (London)* **394,** 784–787.
6. Roelfsema, P. R., Lamme, V. A. & Spekreijse, H. (1998) *Nature (London)* **395,** 376–381.
7. Singer, W. & Gray, C. M. (1995) *Annu. Rev. Neurosci.* **18,** 555–586.
8. Van Essen, D. C. & Maunsell, J. H. R. (1983) *Trends Neurosci.* **6,** 370–375.
9. Salin, P.-A. & Bullier, J. (1995) *Physiol. Rev.* **75,** 107–154.
10. Olson, C. & Lawler, K. (1987) *J. Comp. Neurol.* **259,** 13–30.
11. Darian-Smith, I., Isbister, J., Mok, H. & Yokota, T. (1966) *J. Physiol. (London)* **182,** 671–689.
12. Ursin, R. & Sterman, M. B. A. (1981) *A Manual for Standardized Scoring of Sleep and Waking States in the Adult Cat* (Brain Information Service, Univ. of California, Los Angeles), pp. 15–23.
13. Tusa, R. J., Palmer, L. A. & Rosenquist, A. C. (1981) in *Cortical Sensory Organization*, ed. Woolsey, C. N. (Humana, Clifton, NJ), pp. 1–31.
14. Bressler, S. L. & Nakamura, R. (1993) *Comput. Neural Syst.* **24,** 515–522.
15. Press, W. H., Teukosky, S. A., Vetterling, W. T. & Flannery, B. P. (1992) *Numerical Recipes in C* (Cambridge Univ. Press, Cambridge, U.K.), pp. 656–706.
16. Perkel, D. H., Gerstein, G. L. & Moore, G. P. (1967) *Biophys. J.* **7,** 419–440.
17. Dummermuth, G., Huber, P. J., Kleiner, B. & Gasser, T. (1971) *Electroencephalogr. Clin. Neurophysiol.* **31,** 137–148.
18. Schanze, T. & Eckhorn, R. (1997) *Int. J. Psychophysiol.* **26,** 171–189.
19. Bressler, S. L., Coppola, R. & Nakamura, R. (1993) *Nature (London)* **366,** 153–156.
20. Steriade, M. & Amzica, F. (1996) *Proc. Natl. Acad. Sci. USA* **93,** 2533–2538.
21. Roelfsema, P. R., Engel, A. K., König, P. & Singer, W. (1997) *Nature (London)* **385,** 157–161.
22. Engel, A. K., Kreiter, A. K., König, P. & Singer, W. (1991) *Proc. Natl. Acad. Sci. USA* **88,** 6048–6052.
23. Nowak, L. G., Munk, M. H. J., Nelson, J. I., James, A. C. & Bullier, J. (1995) *J. Neurophysiol.* **74,** 2379–2400.
24. Frien, A., Eckhorn, R., Bauer, R., Woelbern, T. & Kehr, H. (1994) *NeuroReport* **5,** 2273–2277.
25. Nowak, L. G., Munk, M. H. J., James, A. C., Girard, P. & Bullier, J. (1999) *J. Neurophysiol.* **81,** 1057–1074.
26. Gray, C. M., König, P., Engel, A. K. & Singer, W. (1989) *Nature (London)* **338,** 334–337.
27. Engel, A. K., König, P., Gray, C. M. & Singer, W. (1990) *Eur. J. Neurosci.* **2,** 588–606.
28. Eckhorn, R. (1994) *Prog. Brain Res.* **102,** 405–426.
29. Rockland, K. S. & Lund, J. S. (1982) *Science* **215,** 1532–1534.
30. Gilbert, C. D. & Wiesel, T. N. (1983) *J. Neurosci.* **3,** 1116–1133.
31. Berger, H. (1929) *Arch. Psychiatr. Nervenkr.* **87,** 527–570.
32. Adrian, E. D. (1947) *The Physical Background of Perception* (Clarendon, Oxford).
33. Gray, C. M., Engel, A. K., König, P. & Singer, W. (1990) *Eur. J. Neurosci.* **2,** 607–619.
34. Williams, T. L., Sigvardt, K. A., Kopell, N. & Remler, M. P. (1990) *J. Neurophysiol.* **64,** 862–871.
35. Rockland, K. S. & Pandya, D. N. (1979) *Brain Res.* **179,** 3–20.
36. Sandell, J. H. & Schiller, P. H. (1982) *J. Neurophysiol.* **48,** 38–48.
37. Mignard, M. & Malpeli, J. G. (1991) *Science* **251,** 1249–1251.
38. Cauller, L. J. & Connors, B. W. (1994) *J. Neurosci.* **14,** 751–762.
39. de Oliveira, S. C., Thiele, A. & Hoffmann, K. P. (1997) *J. Neurosci.* **17,** 9248–9260.
40. Singer, W. (1993) *Annu. Rev. Physiol.* **55,** 349–374.
41. Markram, H., Lubke, J., Frotscher, M. & Sakmann, B. (1997) *Science* **275,** 213–215.
42. Bernasconi, C. & König, P. (1999) *Biol. Cybern.* **8,** 199–210.
43. Bernasconi, C., von Stein, A., Chiang, C. & König, P. (2000) *NeuroReport* **11,** 689–692.
44. Bullock, T. H., Achimowicz, J. Z., Duckrow, R. B., Spencer, S. S. & Iragui-Modoz, V. J. (1997) *Electroencephalogr. Clin. Neurophysiol.* **103,** 661–678.
45. Kopell, N., Ermentrout, G. B., Whittington, M. A. & Traub, R. D. (2000) *Proc. Natl. Acad. Sci. USA* **97,** 1867–1872.
46. Lopes da Silva, F. H. & Storm van Leeuwen, W. (1977) *Neurosci. Lett.* **6,** 237–241.
47. Chatila, M., Milleret, C., Buser, P. & Rougeul, A. (1992) *Electroencephalogr. Clin. Neurophysiol.* **83,** 217–222.
48. Orban, G. A. (1995) *Neuronal Operations in the Visual Cortex* (Springer, Heidelberg), pp. 47–53.
49. Silva, L., Amitai, Y. & Connors, B. (1991) *Science* **251,** 432–435.
50. Arieli, A., Shoham, D., Hildesheim, R. & Grinvald, A. (1995) *J. Neurophysiol.* **73,** 2072–2093.
51. Arieli, A., Sterkin, A., Grinvald, A. & Aertsen, A. (1996) *Science* **273,** 1868–1871.
52. Gray, C. M. & McCormick, D. A. (1996) *Science* **274,** 109–113.
53. Llinas, R. R. (1988) *Science* **242,** 1654–1664.